1981ApJ...245.1043Y

THE ASTROPHYSICAL JOURNAL 245:1043–1053, 1981 May 1
© 1981. The American Astronomical Society. All rights reserved. Printed in U.S.A.

AM HERCULIS: THE MAGNETIC MAW UNCLOAKS ITSELF

PETER YOUNG AND DONALD P. SCHNEIDER
Palomar Observatory, California Institute of Technology
AND
STEPHEN A. SHECTMAN
Mount Wilson and Las Campanas Observatories, Carnegie Institution of Washington
Received 1980 September 2; accepted 1980 November 3

ABSTRACT

We have obtained a complete orbit of spectroscopy at 2.3 Å resolution on AM Herculis in its low state. We find:

1. Strong, sharp Hβ, Hγ, and Hδ lines and weak, sharp He I λλ4471, 4922, and 5015 lines. The He II λ4686 line is also weak and sharp. There is no trace of the broad emission component present at high state. The radial velocity amplitude $K = 79$ km s^{-1} and fiducial phase $\phi_0 = 0.61$ identify the sharp emission as being related to the sharp emission component seen at high state.

2. The spectrum is stuffed with broad absorption troughs flanking the Balmer lines. These troughs are 10% deep, 80 Å wide, and vary in strength with orbital phase (being strongest at $\phi_{mag} = 0.6$). The troughs show internal structure and are identified as being Zeeman-shifted multiplets of Hβ, Hγ, and Hδ seen in a magnetic field of 1.3×10^7 gauss. The trough structure allows us to place a limit of 10^6 gauss in the variation of the magnetic field in the absorption region. This suggests the lines arise from the accreting polar cap of the white dwarf.

3. Lower resolution (13 Å) spectra in the red show strong, narrow Hα emission. The energy distribution rises sharply longward of 6500 Å, and there are broad, deep TiO bands from the M4.5 V red dwarf in the binary system. The Zeeman components of Hα are confused with some of these TiO bands.

Subject headings: stars: binaries — stars: individual — stars: magnetic — stars: white dwarfs

I. INTRODUCTION

AM Herculis (alias 3U 1809+50) is the prototype of a new class of nova-like binary star systems. Its extraordinary nature was evident when large optical circular polarization was discovered by Tapia (1977).

The system has two "states," and it spends most of its time in the high state at V magnitude 13. Upon occasion AM Herculis slips into a low state at V magnitude 15 where it enjoys a brief sojourn. Although comprehensive spectroscopy has been done in the high state by Stockman *et al.* (1977), Greenstein *et al.* (1977, hereafter GSBB), and Young and Schneider (1979, hereafter YS), there is no good spectroscopy of the low state.

We were alerted to the onset of a new low state in 1980 May by the indefatigable members of the American Association of Variable Star Observers (Mattei *et al.* 1980) and were fortunate to find AM Herculis ensconced in this low state for our observing run.

II. OBSERVATIONS

We observed a complete 3.09 hour orbit of AM Herculis from 1980 August 1.156 UT to 1.299 UT with the Reticon photon counting detector on the Cassegrain digital spectrograph of the 200-inch (5.08 m) telescope. Two slits of 0.″9 by 4″ were used to observe object and sky simultaneously in the two sides of the Reticon array. A 1200-line grating gave a dispersion of 45 Å mm^{-1}, a spectral resolution of 2.3 Å (FWHM), and wavelength coverage from 3980 Å to 5050 Å. The observations were of 500 seconds each. We made frequent breaks to observe an inert gas lamp (He-Ar) to establish the wavelength scale; these breaks were 100 seconds long between pairs of 500 second integrations.

In Figure 1 we show the 21 spectra summed to show the mean low-state spectrum of AM Herculis. The spectra were shifted into the moving frame of the emission lines prior to their addition. The Balmer lines are rampant, but He I λ4471 and He II λ4686 are in a sorry condition compared with their high-state strength. The spectrum in Figure 1 exhibits lumpiness on a scale of 3 pixels, and the lumps are statistically significant. The whole region is bristling with a thicket of tiny emission lines. Only the strongest lines are identified in Figure 1 and Table 1.

It is rather difficult to distinguish the tiny emission lines from the broad, structured absorption troughs also present in the spectrum. Particularly strong troughs are seen at λ4660, λ4820, and λ4940, with the latter two troughs apparently showing some internal structure. Other troughs are seen flanking Hγ and Hδ, but these are badly infested with minute emission lines, which makes it difficult to define a continuum.

We made additional observations in the red with the 200-inch (5.08 m) telescope using the PFUEI prime focus CCD camera/spectrograph. At a dispersion of 440 Å

© American Astronomical Society • Provided by the NASA Astrophysics Data System

1981ApJ...245.1043Y

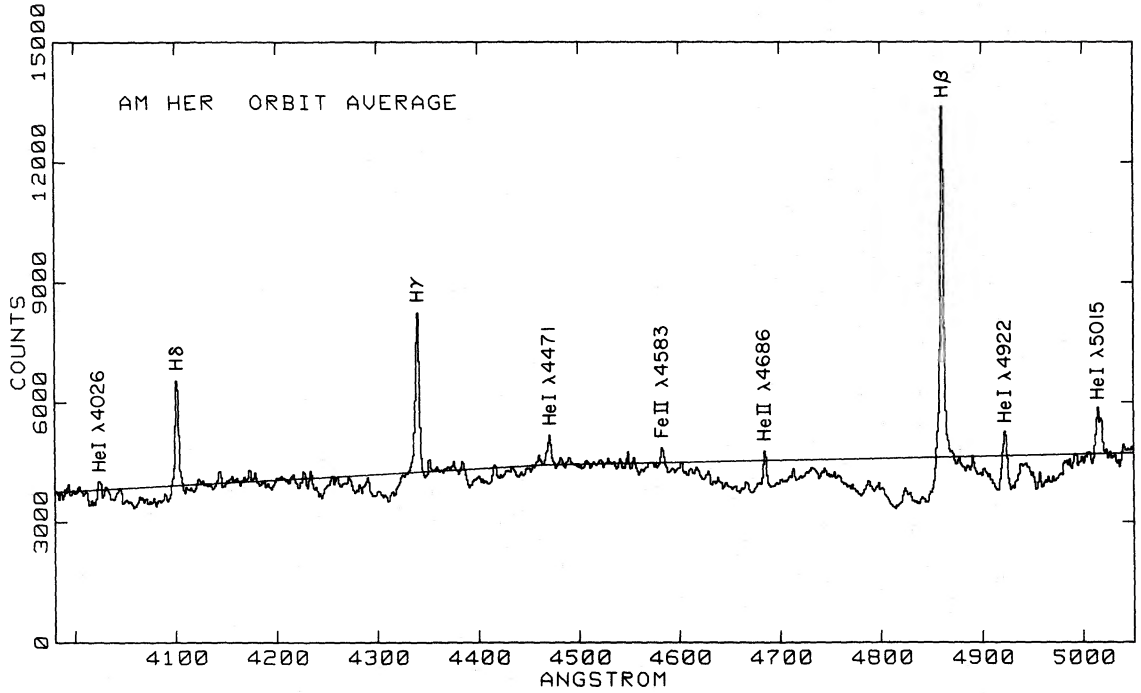

FIG. 1.—AM Her spectra summed. The spectra were shifted into the moving frame of the sharp emission lines prior to their addition. The stronger emission lines are marked; many other tiny lines infest the spectrum as well as the broad absorption troughs around the Balmer lines. The continuum used to define emission line equivalent widths is marked. The data are on a linearized flux scale with 1 count as $AB_\nu = 24$. Each bin is 1.19 Å and the instrumental resolution is 2.3 Å.

mm^{-1} and using a 0".5 by 180" slit, we obtained spectral resolution of 13 Å covering the range 4550 Å to 7700 Å. The detector was a 500 by 500 pixel, low-noise, Texas Instruments CCD array. The CCD is thinned to 7 μm, is used in a back-illuminated mode, and is cooled to $-130°$ C using liquid nitrogen. Three integrations of 1800 seconds each were made from 1980 August 23.152 UT to August 23.217 UT. Helium lamps and sky lines were used to determine the wavelength scale. These observations will be discussed further in § IV.

Since the low state allows the red dwarf to compete more favorably with the accretion luminosity, Hutchings, Crampton, and Cowley (1980, hereafter HCC) were able to present new dynamical information on the secondary. Their data indicate that the configuration of YS is incorrect in both the red dwarf orbital velocity amplitude

TABLE 1

STRONG EMISSION LINES IN AM HERCULIS

Line	Equivalent Width (Å)	Continuum[a] AB_ν magnitude	FWHM (km s^{-1})	Flux (ergs cm^{-2} s^{-1})
He I λ4026	0.54	15.05	...	3.5×10^{-15}
Hδ	3.43	15.03	215	2.1×10^{-14}
Hγ	4.32	14.93	210	2.7×10^{-14}
He I λ4471	0.76	14.88	230:	4.6×10^{-15}
Fe II λ4583	0.48	14.87	170:	2.8×10^{-15}
He II λ4686	0.67	14.86	120:	3.8×10^{-15}
Hβ	9.67	14.84	180	5.2×10^{-14}
He I λ4922	1.75	14.84	270:	9.1×10^{-15}
He I λ5015	1.58	14.83	320:	8.0×10^{-15}
Fe II λ5170[b]	0.97	14.94	...	4.2×10^{-15}
He I λ5875[b]	4.20	15.04	...	1.3×10^{-14}
Hα[b]	42.10	14.71	...	1.4×10^{-13}
He I λ6678[b]	2.10	14.83	...	6.0×10^{-15}
He I λ7065[b]	2.60	14.48	...	9.2×10^{-15}

[a] $AB_\nu = -2.5 \log_{10} f_\nu - 48.60$.
[b] From PFUEI spectra.

© American Astronomical Society • Provided by the NASA Astrophysics Data System

1981ApJ...245.1043Y

(nearly a factor of 3 too large) and the red dwarf phasing (160° too late). In § V we present rather old but unpublished data acquired with the same procedure as given in YS. These measurements were originally made merely to check the claims of YS; it now appears there is strong justification for their presentation.

III. EMISSION LINES

a) *The Period*

From Olson (1977) we find the time of photometric minimum of AM Herculis to have occurred at

$$\text{HJD} = 2443014.7133 \pm 0.0008 . \quad (1)$$

The latest photometric observations of AM Herculis at maximum are by Bailey and Axon (1980). From measuring their plot we find the photometric minimum to be at

$$\text{HJD} = 2444133.0254 \pm 0.0010 . \quad (2)$$

This gives a period (with 8674 cycles) of

$$P = 0.12892691 \pm 0.00000015 . \quad (3)$$

We shall continue to use the standard ephemeris for magnetic phase ϕ_{mag} given by

$$\text{HJD} = 2443014.765 + 0.128927E , \quad (4)$$

since the period in equation (3) does not differ detectably from that in equation (4). Photometric minimum is then at $\phi_{\text{mag}} = 0.5990$. It is to be noted that the mean photometric minima in YS occurred at $\phi_{\text{mag}} = 0.624$. This suggests either period changes or, more probably, that the photometric minimum drifts slightly in binary phase. Since the light curve (see Fig. 2) no longer presents a well-defined photometric minimum, we have no way to check whether equation (4) is still valid.

b) *Emission Line Radial Velocities*

The lines present at minimum light are quite sharp with (corrected) FWHM widths of 200 km s^{-1}. The sharp component seen previously by GSBB and YS has an FWHM of only 110 km s^{-1}, although it was mainly the He I lines rather than the Balmer lines that were observed. The software package ANTARES was used to determine the emission line radial velocities and to fit the relation

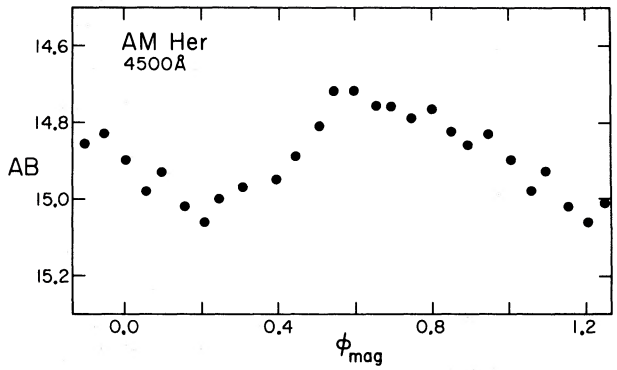

FIG. 2.—Cassegrain slit photometry of AM Her. The *AB* magnitude at 4500 Å in the continuum is plotted as a function of magnetic phase ϕ_{mag}.

$$V = \gamma + K \sin 2\pi(\phi_{\text{mag}} - \phi_0) \quad (5)$$

to create the values displayed in Table 2. Only the Balmer-line radial velocities are accurate; the He I and He II lines were all weak and gave poor results. In Figure 3 we show the radial velocity curve of Hβ. We note that:

1. The phase $\phi_0 = 0.608$ shows the emission lines present at minimum to be associated with the sharp component of GSBB and YS. The broad component is not present. The fiducial phases found by GSBB and YS for the sharp components were about 0.67.
2. The radial velocity amplitude $K = 79$ km s^{-1} is somewhat lower than the value of 117 km s^{-1} for the He I sharp component at maximum (GSBB, YS) but the same as that found by GSBB for the He II λ4686 line (76 km s^{-1}).
3. The γ velocity of -19 km s^{-1} is in good agreement with previous values.
4. Our epoch of velocity $V = \gamma$ traveling from blue to red is

$$\text{HJD} = 2444452.7662 \pm 0.0005 . \quad (6)$$

Unfortunately, K, γ, and ϕ_0 values of the Balmer lines for the high state were not measured (although GSBB

TABLE 2

RADIAL VELOCITIES IN AM HERCULIS

Line	K (km s^{-1})	γ (km s^{-1})	ϕ_0 (magnetic)	σ(O − E) (km s^{-1})
Hδ	77 ± 4	−14 ± 4	0.607 ± 0.008	11
Hγ	80 ± 4	−25 ± 4	0.608 ± 0.007	12
He I λ4471	81 ± 12	−40 ± 15	0.510 ± 0.040	36
He II λ4686	50 ± 10	−32 ± 9	0.624 ± 0.030	29
Hβ	80 ± 3	−19 ± 3	0.609 ± 0.007	11
He I λ4922[a]	59 ± 10	30 ± 10	0.618 ± 0.007	33
Mean Balmer	79 ± 2	−19 ± 2	0.608 ± 0.004	...

[a] This line is buried in a thicket of Zeeman-shifted Hβ absorption, which may explain the discrepant γ velocity.

© American Astronomical Society • Provided by the NASA Astrophysics Data System

1981ApJ...245.1043Y

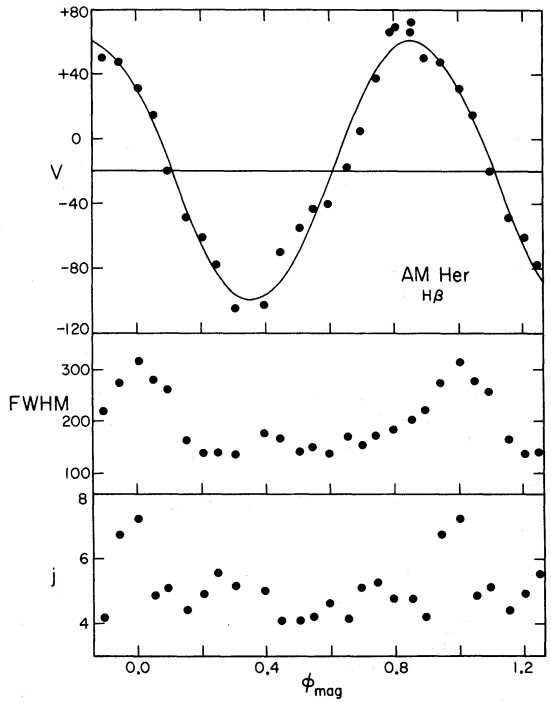

FIG. 3.—Hβ emission in AM Her. The top graph shows the line velocity V km s^{-1} versus magnetic phase ϕ_{mag}. The γ velocity of -19 km s^{-1} and the best fitting circular orbit are shown. The center section shows the FWHM of the line in km s^{-1}. The lowest section shows the line flux j in units of 10^{-14} ergs cm^{-2} s^{-1}.

show a spectrum of Hα which shows the presence of a sharp component in the high state). Our values of K, γ, and ϕ_0 for the He I and He II lines in the low state are not reliable because of the weakness of those lines. A direct comparison of the sharp emission in the high and low states is not possible. The sharp components visible at high and low states are probably not the same because of the different radial velocity amplitudes and slightly different phasing. Moreover, from Figure 3 we see that the line flux in the low-state sharp component does not vary much with orbital phase. Both GSBB and YS found the high-state sharp component to have much more dramatic variations in strength with orbital phase, presumably as the emitting hemisphere of the red dwarf rotated in and out of view.

IV. ABSORPTION TROUGHS

a) Orbital Variations

Figure 1 shows absorption troughs averaged over an orbital cycle. In Figure 4 we show observations summed to give 10 spectra per orbit. The troughs vary markedly in character with orbital phase as follows:

1. At orbital phase 0.6, the troughs are strongest and show internal structure. There are troughs at λ4050, λ4300, λ4420, λ4660, λ4810, and λ4920. The trough at λ4660 is smooth, but the others show varying degrees of internal structure (especially the λ4810 and λ4920 features). There are other small absorption features between the Hγ and Hδ emission lines.

2. At orbital phase 0.1, the troughs are virtually invisible. Instead, the continuum around Hβ shows a shallow, very wide (300 Å) depression. There are still hints of structured absorption shortward of Hγ and Hδ, and on both sides of Hβ.

3. The shape and position of the trough structure shows little change with orbital phase; it changes only in strength. This is best seen in the λ4770, λ4810, and λ4840 subcomponents in the trough just shortward of Hβ.

We have not conducted a radial velocity study of the troughs since the next section demonstrates that there is no sense in doing so. We note, though, that the subtroughs hold their position to within 1 Å when they are visible.

The idea that the absorption features may arise from the cool secondary star was briefly entertained. A casual rumination reveals the notion to be ridiculous for the following reasons:

1. According to YS the red dwarf is much too faint and red to be visible at 4500 Å, even in the low state.

2. The absorption troughs are too wide for M dwarf lines and, moreover, are in the wrong places to be the usual band structures.

b) Zeeman Multiplet Identifications

The presence of the three troughs around Hβ strongly resembles the complex Paschen-Back splittings of a normal Hβ Zeeman triplet (see Garstang 1977; Kemic 1974). The complicated arrays of line positions for Hβ (and other H and He lines) are given in Kemic (1974). We may deduce immediately from the general positions of the troughs around Hβ that the magnetic field strength must be somewhat over 10^7 gauss. This is sufficiently strong that the quadratic Zeeman shifts move all components shortward (which is why the central Zeeman component is shortward of Hβ). Small variations in the magnetic field in the emitting region will blur individual transitions more in the λ4660 trough than in the λ4810 and λ4920 troughs since the derivatives $d\lambda/dB$ are highest for the lines in that trough.

In order to illustrate the Zeeman splitting of the Balmer lines, we have taken a magnetic field distribution function

$$p(B) = \exp\left[-(B - B_0)^2/2\sigma_B{}^2\right]/\sigma_B(2\pi)^{1/2}\,, \qquad (7)$$

and computed the multiplet strength S_ν per unit frequency using the data of Kemic (1974). We have then computed an absorption optical depth $\tau_\nu \propto \nu S_\nu$ and taken $1 - e^{-\tau_\nu}$. The strength seen will actually depend in a nightmarish way on the atomic level population and radiative transfer effects. However, our calculation will serve to show the expected position and spread in the absorption features.

In Figure 5 we show a comparison between an AM Herculis spectrum and the magnetic Balmer features with

$$B_0 = 1.3 \times 10^7 \text{ gauss}\,,$$
$$\sigma_B = 10^6 \text{ gauss}\,. \qquad (8)$$

© American Astronomical Society • Provided by the NASA Astrophysics Data System

1981ApJ...245.1043Y

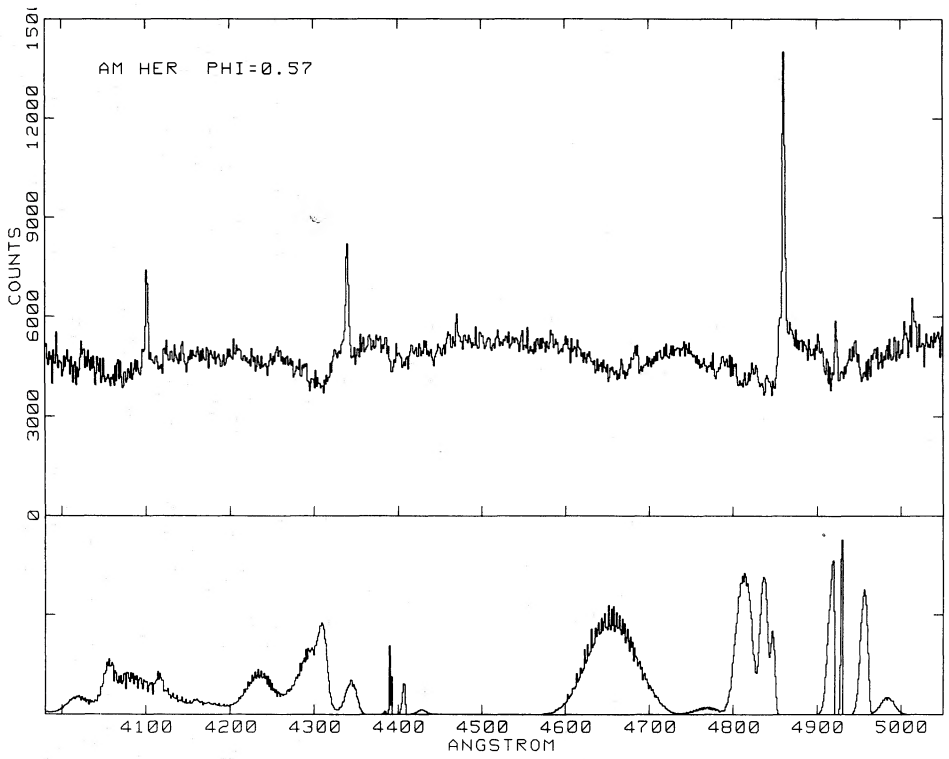

FIG. 5.—Comparison of absorption spectrum of AM Her at phase 0.57 with expected absorption from Zeeman-shifted Balmer lines. We have used a mean magnetic field strength of 1.3×10^7 gauss and a standard deviation spread of 10^6 gauss. The theoretical plot shows $1 - e^{-\tau_\nu}$ for the Zeeman-split components of Hβ, Hγ, and Hδ; optical depth 0.75 pertains to the center of the λ4660 trough (which is not this deep in the data if only ~ 20% of the continuum flux is from the Zeeman absorption region). The position of the Zeeman absorption features in the AM Her spectrum is correct; some of the strengths are discrepant probably because we have not done a full solution to the radiative transfer problem. Bristles on the theoretical Zeeman troughs are an artifact of the discrete numerical integration.

The correspondence between individual features in the observed and calculated spectra shows magnetically afflicted Balmer features to be a satisfactory explanation for the absorption troughs in AM Herculis.

The field strength required is quite accurately determined, mainly from the position of the λ4660 trough. This moves very rapidly with changing magnetic field; we would put an estimated uncertainty of only 5×10^5 gauss on the value B_0. A small spread in field strength is required to blur the individual transitions in the λ4660 trough. This must not be too large or else the internal structure in the other troughs is blurred. We would estimate that 5×10^5 gauss $< \sigma_B < 1.5 \times 10^6$ gauss. The lack of change in the trough positions with orbital phase demands that B_0 not change by more than 5×10^5 gauss around the orbit. There is no evidence for any absorption in a field of greater than 1.5×10^7 gauss.

c) *The Red Spectra*

The three observations made with the PFUEI were at orbital phases $\phi_{\rm mag} = 0.45, 0.62$, and 0.79. The sum of the three spectra, taken at orbital phases when the Zeeman absorption troughs are strongest, are shown in Figure 6. Strong, sharp emission lines of H and He I are visible; equivalent widths and strengths are given in Table 1. The Hβ Zeeman troughs are visible in Figure 6, although the spectral resolution (at the end of the spectrum) is insufficient to resolve their internal structure. Also visible longward are a number of troughs, at 6250 Å, 6800 Å, 7200 Å, and 7600 Å, and a sharp rise in the continuum flux longward of 6500 Å. The absorption troughs in the red are clearly those of the red dwarf component of the binary system first discovered by YS. The depth of the TiO bands indicates a spectral type of M4.5 V as was found by YS; the star dominates the spectrum longward of 7000 Å. The Zeeman components of Hα are, unfortunately, confused with the TiO bands at 6250 Å and 6800 Å, and it is not possible to seperate them without creating ambiguity. Spectropolarimetry would be of use here; in this case it would be able to provide more information than simply the sign of the magnetic field. The Zeeman components in Figure 6 show, however, that the troughs flanking Hα emission are in the correct location for the Zeeman absorption components in a magnetic field of 1.3×10^7 gauss, although TiO must also be present.

V. THE DYNAMICS OF THE SECONDARY

In 1978 October we obtained high resolution near-infrared spectra of AM Herculis in the high state. (See YS for a description of the instrumentation and the reduction procedures.) The observations were made on two nights,

© American Astronomical Society • Provided by the NASA Astrophysics Data System

1981ApJ...245.1043Y

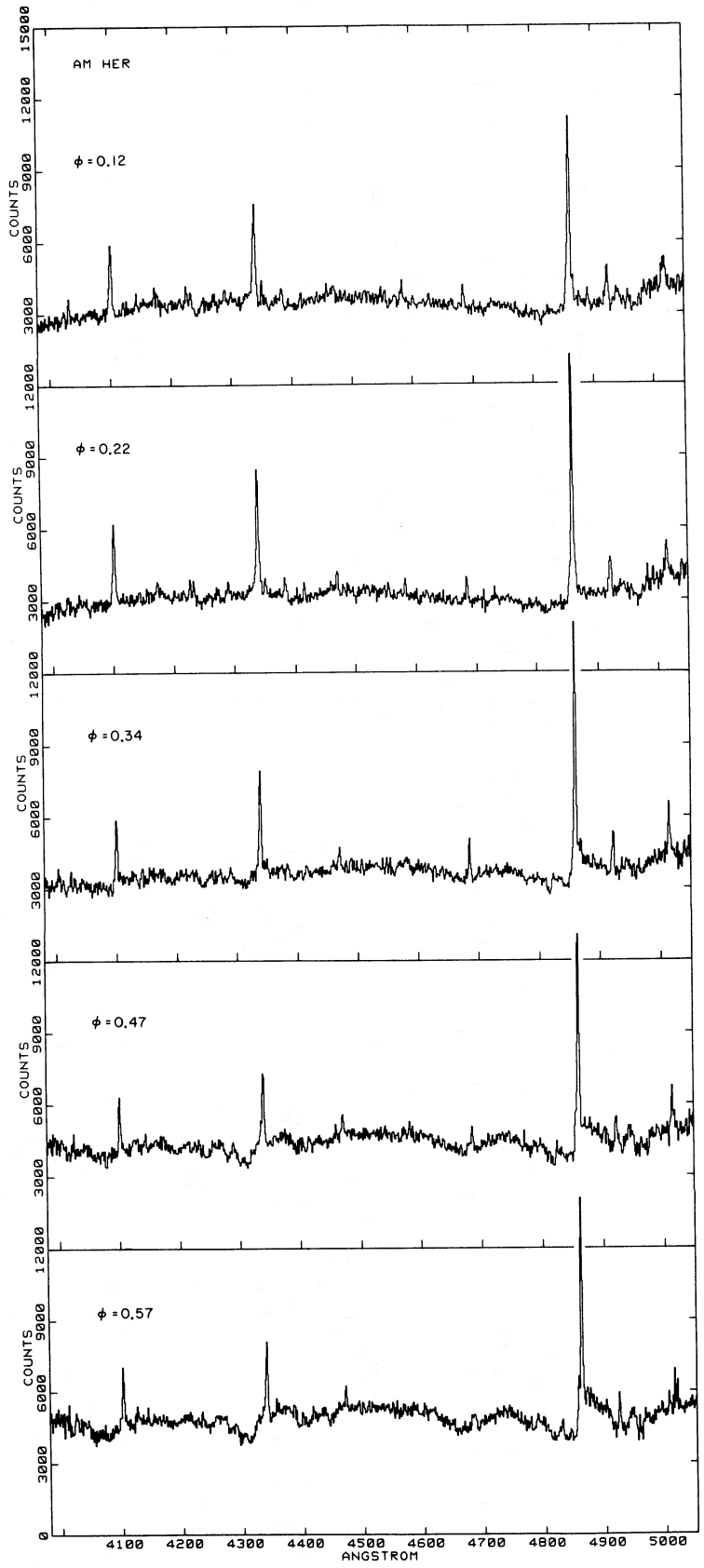

FIG. 4.—A complete orbit of AM Her spectra. All spectra are on the same linearized flux scale with 1 data number corresponding to $AB_\nu = 24$. Each bin is 1.19 Å and the instrumental resolution is 2.3 Å. Magnetic phase ϕ is shown next to each of the 10 spectra.

© American Astronomical Society • Provided by the NASA Astrophysics Data System

1981ApJ...245.1043Y

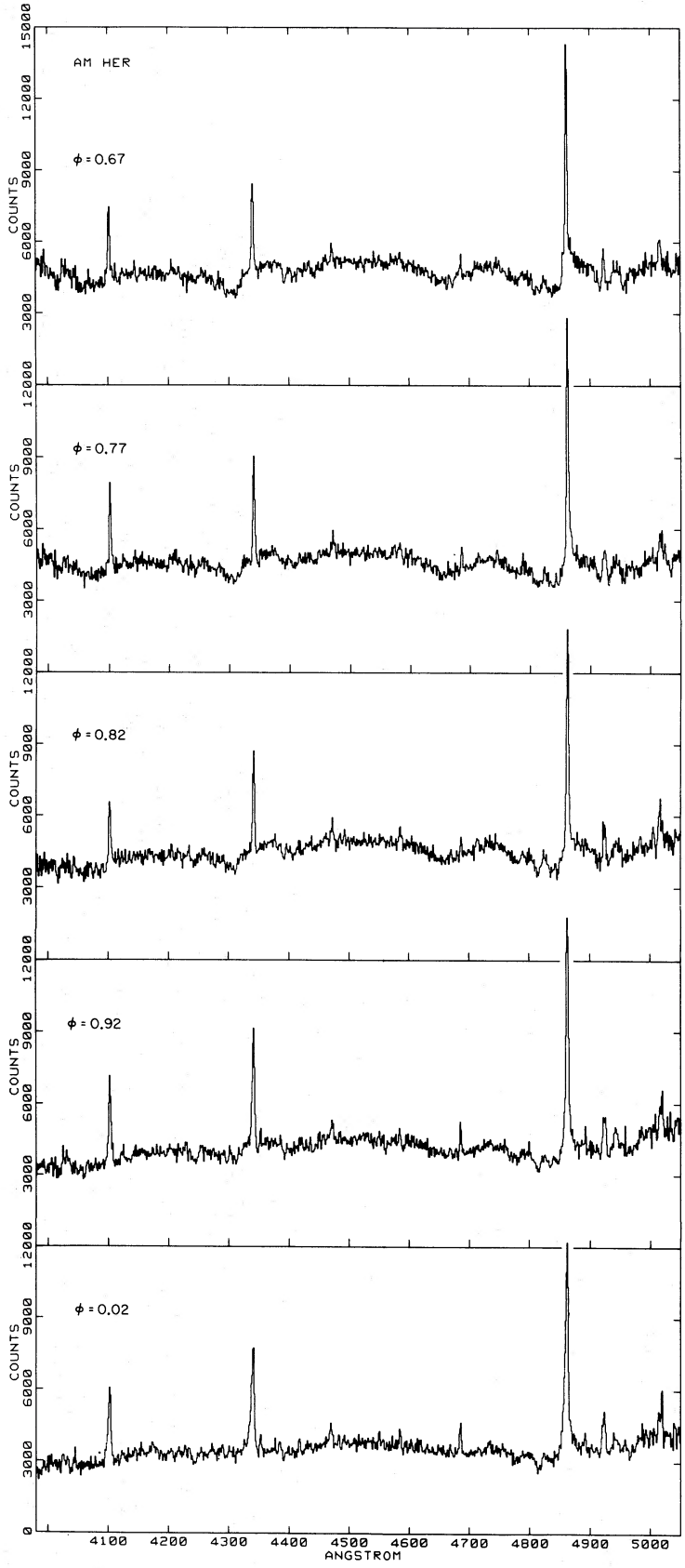

FIG. 4.—*Continued*

© American Astronomical Society • Provided by the NASA Astrophysics Data System

1981ApJ...245.1043Y

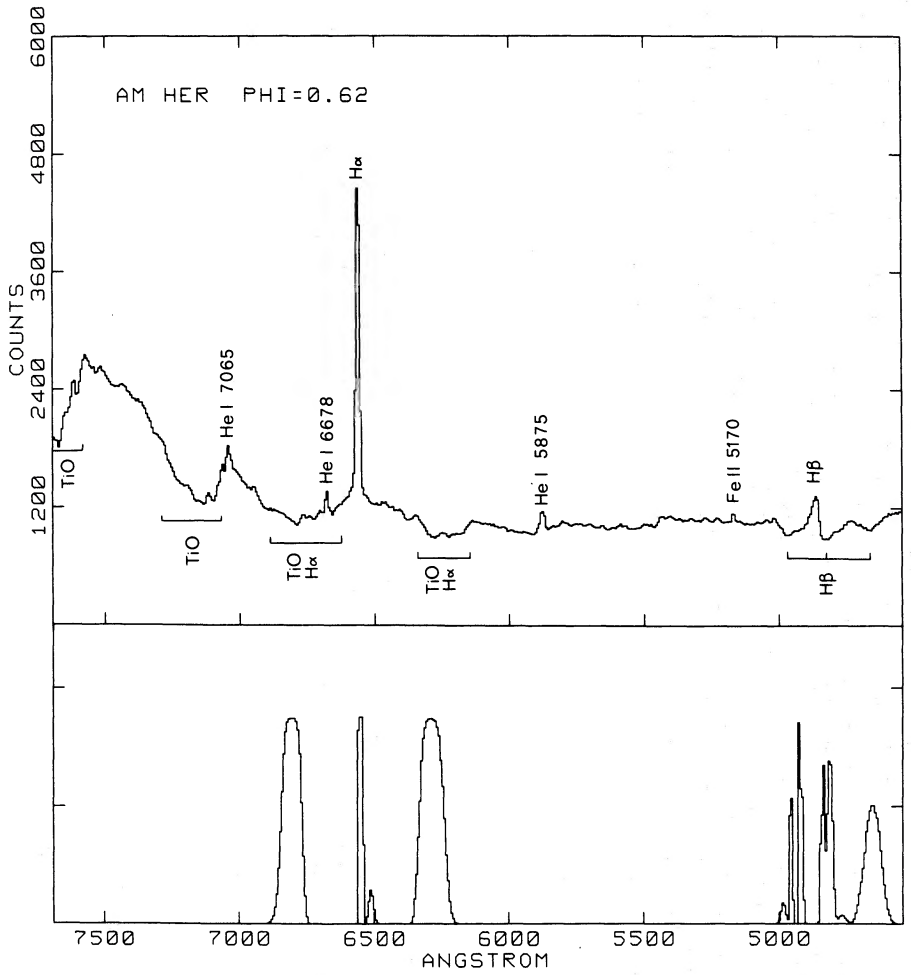

FIG. 6.—PFUEI spectrum of AM Her at phase 0.62, together with expected positions of absorption from Zeeman-shifted Balmer lines. The magnetic field strength is 1.3×10^7 gauss and has a standard deviation spread of 10^6 gauss, as in Fig. 5. The instrumental resolution on AM Her is 13 Å, and the data are on a linearized flux scale with 1 data number being $AB_v = 22.5$. The Hβ Zeeman triplet is clearly visible, but the Hα absorption features are confused with the TiO bands from the red dwarf star and also with the strong Hα emission.

7.107–7.268 October and 10.112–10.247 October (UT). The Mount Wilson 100-inch (2.54 m) coudé spectrograph/Reticon detector had a dispersion of 40 Å mm^{-1}, resolution of 2 Å, and spectral coverage of 7700–8700 Å. The summed spectrum is displayed in Figure 7. There are a few striking differences from the spectra in 1978 May and July (YS). Emission from O I, He II, and the Paschen series are prominent in the October spectrum; they were nonexistent in the YS data.

Using plates acquired during the 1980 low state, HCC were able to measure sharp absorption features from the red dwarf. The resulting k_R (68 km s^{-1}) and fiducial phase ϕ_0 (0.18) are in serious disagreement with YS ($k_R = 175$ km s^{-1}, $\phi_0 = 0.63$).

The October Mount Wilson data was phased using parameters from YS and HCC; the results are shown in Figure 8. The top panel in the figure gives a M4.5 V standard for comparison. The appearance of the Na I λ8183–94 lines is clearly superior with the YS phasing, where a cleanly split doublet of respectable strength appears. Only a vague depression in the vicinity of the Na I lines is visible in the HCC model. The best results for the data) is 190 ± 30 km s^{-1}. It is not clear what 200 km s^{-1}. Our current best estimate of k_R (including all the data) is 190 ± 30 km s^{-1}. It is not clear what ARCTURUS is homing in on; in the event that the absorption features are real, they present a new and puzzling aspect of the system.

VI. DISCUSSION

The small spread in magnetic field strength in the region responsible for the absorption troughs in AM Herculis indicates that we are probably seeing the surface of the white dwarf. In a dipole field

$$B_r = B_*(r_*/r)^3 \cos\theta$$
$$B_\theta = (B_*/2)(r_*/r)^3 \sin\theta\,, \qquad (9)$$

© American Astronomical Society • Provided by the NASA Astrophysics Data System

1981ApJ...245.1043Y

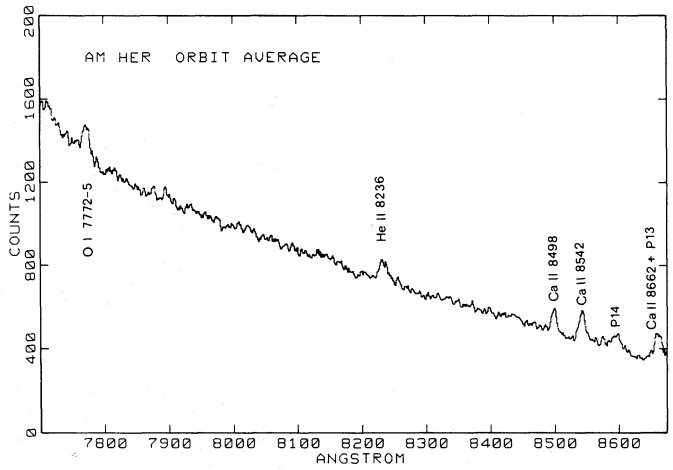

FIG. 7.—Mount Wilson coudé data on AM Her in the high state in 1978 October. Each data bin is 1.3 Å and the spectral resolution is 2 Å. The data are not on a flux scale.

we would have $B_* = 1.3 \times 10^7$ gauss on the surface of the dwarf, at the pole ($r = r_*$, $\theta = 0$). Since the field strength is then

$$B = B_*\left(\frac{r_*}{r}\right)^3\left\{\frac{1}{4}\sin^2\theta + \cos^2\theta\right\}^{1/2}, \qquad (10)$$

in order to avoid excessive spread in the field strength we must have

$$0 \leq \theta < 25°$$

or

$$1 \leq r/r_* < 1.025 \qquad (11)$$

in the region responsible for the absorption. We think it likely that the accreting polar cap alone contributes much of the luminosity, more so per unit area than the rest of the white dwarf surface. Accretion onto the magnetic pole is channeled down field lines, and the area of the funnel varies as

$$A(r) = A_*\left(\frac{r}{r_*}\right)^3\left\{\cos^2\theta + \frac{1}{4}\sin^2\theta\right\}^{-1/2}. \qquad (12)$$

The field lines can hardly connect to more than an area defined by the whole hemisphere of the red dwarf companion. Channeled down a dipole field from $r = 10^{11}$ cm to $r = 10^9$ cm, this implies the polar cap suffering accretion has $\theta \leq 3°$. The spread in magnetic field strength may be caused by radial radiative transfer up the column (note that in this case $r/r_* - 1 \sim \theta_{cap}$, indicating a "pillbox" region of comparable height and width).

If the luminous region emits thermally and contributes $\sim 20\%$ of the continuum in the optical blue portion of the spectrum, then (for a distance of 70 pc to AM Herculis) the required relation between area and temperature is

$$(A/10^{16}\ \mathrm{cm}^2) = (T/10^6\ \mathrm{K}), \qquad (13)$$

leading to $T \sim 10^6$ K if just the polar cap ($\theta < 3°$) is emitting. This must be considered unpleasant in view of the presence of neutral hydrogen. Temperatures down to 10^4 K can be obtained by enlarging the area to 10^{18} cm^2 and having radiation from $\theta \leq 25°$ (which still allows a luminosity contrast between the cap and the rest of the white dwarf's photosphere). The problem is then how to explain why the cap should be luminous to such a large extent when funneled gas can only impact in $\theta \leq 3°$, unless the gas can spread laterally across the field lines as it is accreted. One possibility might be radiative heating of the white dwarf pole by the luminosity of the accretion column itself.

Since the absorption troughs are most prominent at phase 0.6, the accreting magnetic pole is presumably towards Earth at this time. The red dwarf is at inferior conjunction at phase 0.63 (YS), so that the accreting pole of the white dwarf is tilted toward the red dwarf. The accreting pole rotates to a little beyond the limb of the white dwarf, judging by the troughs which just manage to disappear at phase 0.1. At this time there is a photometric minimum (see Fig. 2), and the absorption troughs have vanished to be replaced with a very wide, shallow continuum depression around Hβ. This may be the rest of the white dwarf glowing dimly with badly smeared Hβ Zeeman lines caused by the variable magnetic field strength over the visible photosphere (from 6.5×10^6 to 1.3×10^7 gauss). We also note that at phase 0.6 the broad emission component (seen in the high state) is redshifted, presumably as material plummets down the magnetic maw. If this scenario is correct, then the primary photometric minimum seen in the high state at phase 0.6 would have to be caused by the cyclotron self-absorption mechanism of Chanmugam and Wagner (1978).

Schneider and Young (1980) gave examples of gas flow in the magnetic dipole geometry for AN UMa and VV Pup. The dipole is probably not a terribly good approximation, since local electric current flows distort the field lines near the red dwarf. Let us explore, however, the consequences of the dipole geometry in AM Herculis.

The major piece of information to be used is the phase offset between the broad emission-line velocities seen at maximum (GSBB, YS) and the red dwarf. The "natural"

© American Astronomical Society • Provided by the NASA Astrophysics Data System

1981ApJ...245.1043Y

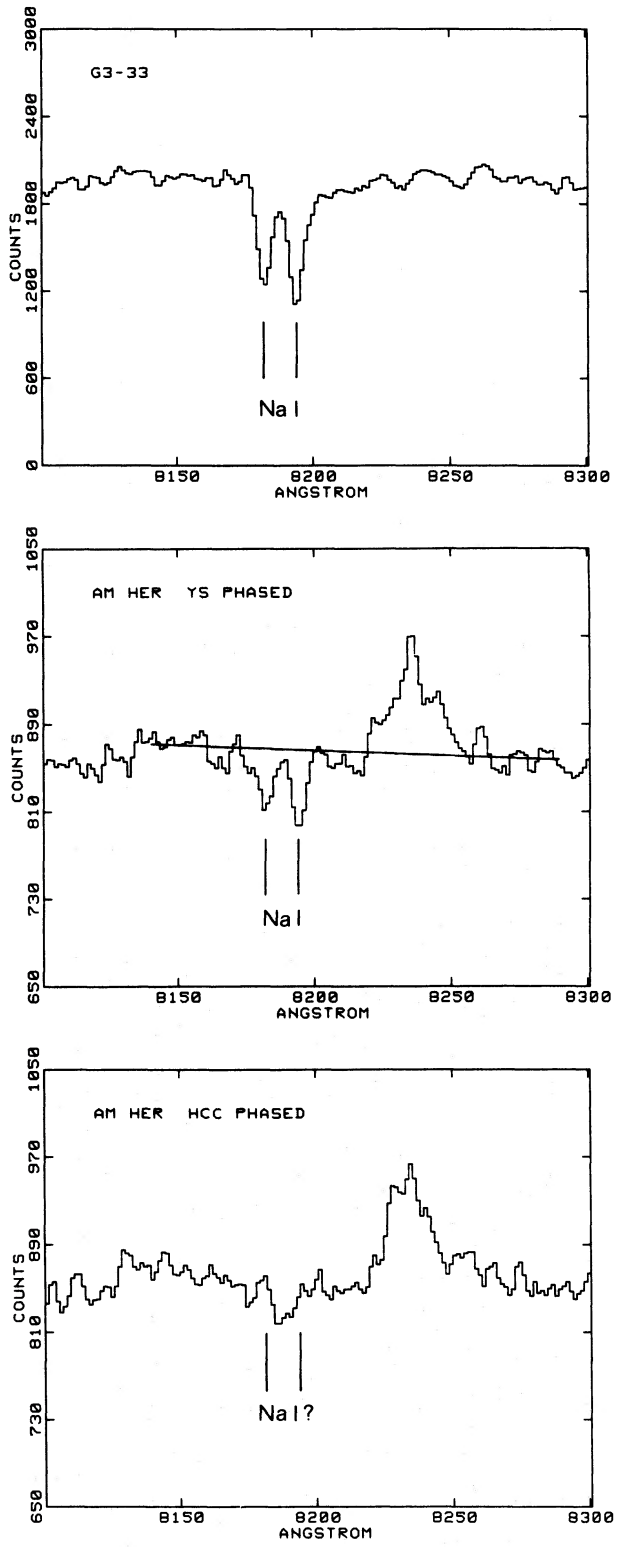

FIG. 8.—Na I λ8183–94 absorption in G3-33 (an M4.5 V star) and in AM Her. The data in Fig. 7 have been phased with the velocity and fiducial phase $k_R = 175$ km s^{-1} and $\phi_0 = 0.63$ found in YS (*middle*); with $k_R = 68$ km s^{-1} and $\phi_0 = 0.18$ which is the red-dwarf motion observed by HCC (*bottom*).

offset is 90° if the broad lines arise from an accretion stream moving from the red to the white dwarf. In VV Pup and AN UMa, this was reduced to 50° by having a large mass-ratio ($q = m_W/m_R$) and by allowing the motion of the gas stream to follow the orbital motion of the red dwarf. In AM Herculis the phase offset is 120°, requiring the gas stream to follow the orbital motion of the white dwarf. This is achieved if the mass ratio is relatively low ($q \lesssim 1.5$).

We now use the velocity and spectral type of the red dwarf to help suggest a mass ratio q. The spectral type of the red dwarf (M4$^+$ V, spectral type refined in Young and Schneider [1980]) yields a mass of 0.22 $M_\odot$ if it is a main-sequence object. It must, at least, obey a normal main-sequence mass-radius relationship (YS). If it is underluminous for its mass, we should demand $m_R > 0.22\ M_\odot$; the work done in the process of mass transfer may consume luminosity (Wade 1980). To lie above the zero-age main sequence, the star must have $m_R < 0.44\ M_\odot$ (YS). Too low a mass ratio q results in too large a value m_R even for high inclinations. We have settled on an illustrative example with

$$\begin{aligned} m_W &= 0.39\ M_\odot \\ m_R &= 0.26\ M_\odot \\ a &= 0.92\ R_\odot \\ r_R &= 0.32\ R_\odot \\ i &= 60°\,, \end{aligned} \tag{14}$$

which fits $P = 0.128927$ days and $k_R = 190$ km s^{-1}. If the magnetic dipole on the white dwarf is tilted 45° over toward the red star (and is not twisted sideways), we obtain a situation where the dipole points nearly toward Earth (angle 15°) at $\phi = 0.63$ and has rotated away from the Earth (angle 105°) at $\phi = 0.13$. This is what is indicated from the visibility of the Zeeman features. The dipole is perpendicular to the line of sight at $\phi = 0.98$ and $\phi = 0.28$. The former perpendicularity corresponds nearly to the linear polarization spike (actually at $\phi = 0$; see Tapia [1977]) seen in the high state. No linear polarization spike is seen at $\phi = 0.28$. The circular polarization (Tapia 1977) is positive from $\phi = 0$ to $\phi = 0.28$ and changes sign at those two phases just as we would expect. The circular polarization is negative from $\phi = 0.28$ to $\phi = 1.0$ with broad eclipse at $\phi = 0.58$ that is attributed to cyclotron self-absorption.

The broad emission lines seen in the high state arise from the accretion column attached to the magnetic pole of the white dwarf tilted toward the red star. This magnetic-dipole gas-stream model gives a predicted fiducial phase $\phi_0 = 0.33$ for the broad emission, with the red dwarf inferior conjunction taken to be $\phi = 0.63$. The observed broad line $\phi_0 = 0.30$ (YS). The narrow emission lines seen in the high state would arise from the surface of the red star as suggested by YS and are eclipsed as the red star rotates. The narrow emission lines seen in the low state are significantly wider than the high state features and have a smaller radial velocity amplitude (79 km s^{-1}

© American Astronomical Society • Provided by the NASA Astrophysics Data System

1981ApJ...245.1043Y

versus 120–150 km s^{-1}). They may arise from a gas cloud enveloping the Roche cusp of the red dwarf; the sharp emission does not suffer strong flux variations around the orbit.

The X-ray data show a mutable eclipse at $\phi = 0.13$ (Hearn and Richardson 1977) which presumably occurs when the accretion pole passes behind the limb of the white dwarf. Changes in the structure of the accretion column can cause this eclipse to disappear, as it does from time to time.

The radius of a 0.39 $M_\odot$ white dwarf would be 0.015 $R_\odot$. With a magnetic field strength of 1.3×10^7 gauss at the pole, we find from equation (10) (for $\theta = 45°$)

$$B(L_1) = 280 \text{ gauss}, \quad (15)$$

and a magnetic-field energy density $B(L_1)^2/8\pi = 3 \times 10^3$ ergs cm^{-3}. The energy density of the gas churning around at the L_1 point is $3\rho kT/2m_H = 210\ (n_H/10^{14}\ cm^{-3})$ ergs cm^{-3} for $T = 10^4$ K. The line widths indicate $n_H < 10^{14}$ cm^{-3} (Stark broadening) and $B(L_1) < 10^5$ gauss (Zeeman broadening). It seems likely, therefore, that $B(L_1)^2/8\pi \gg 3\rho kT/2m_H$ and that the magnetic field dominates the gas flow even at the L_1 point. These considerations are terribly sensitive to the geometry of the two stars since a factor $(r_*/r_{L_1})^6$ enters into the magnetic energy density. It does seem highly unlikely that a true accretion disk can form in the system.

We thank Jesse Greenstein for suggesting the Zeeman splitting interpretation of the absorption troughs and directing us to the theoretical literature. We thank Gary Yanik for assistance with the photon counting detector, and Juan Carrasco and Bruce Cuney for efficient operation of the Hale reflector. This work was supported in part by the National Science Foundation grant AST 80-03398.

REFERENCES

Bailey, J., and Axon, D. J. 1980, *M.N.R.A.S.*, **194**, 187.
Chanmugam, G., and Wagner, R. L. 1978, *Ap. J.*, **222**, 641.
Garstang, R. H. 1977, *Rept. Progr. Phys.*, **40**, 105.
Greenstein, J. L., Sargent, W. L. W., Boroson, T. A., and Boksenberg, A. 1977, *Ap. J. (Letters)*, **218**, L121 (GSBB).
Hearn, D. R., and Richardson, J. A. 1977, *Ap. J. (Letters)*, **213**, L115.
Hutchings, J. B., Crampton, D., and Cowley, A. P., 1980, preprint ("Optical Spectroscopy of AM Her: The 1980 Low State") (HCC).
Kemic, S. B. 1974, JILA Report No. 113 (Boulder: Colorado Assoc. University Press).
Mattei, J., Morgan, J., Bois, B., Mayer, E., Griesé, J., and Scovil, C. 1980, *IAU Circ.*, No. 3490.
Olson, E. C., 1977, *Ap. J.*, **215**, 166.
Schneider, D. P., and Young, P. J. 1980, *Ap. J.*, **240**, 871.
Stockman, H. S., Schmidt, G. D., Angel, J. R. P., Liebert, J., Tapia, S., and Beaver, E. A. 1977, *Ap. J.*, **217**, 815.
Tapia, S. 1977, *Ap. J. (Letters)*, **212**, L125.
Wade, R. A. 1980, Ph.D. thesis, California Institute of Technology.
Young, P., and Schneider, D. P. 1979, *Ap. J.*, **230**, 502 (YS).
———. 1980, preprint ("A Quest for the Red Companion in Six Cataclysmic Binaries").

DONALD P. SCHNEIDER and PETER YOUNG: Robinson Laboratory of Astrophysics, 105-24, California Institute of Technology, Pasadena, CA 91125

STEPHEN A. SHECTMAN: Mount Wilson and Las Campanas Observatories, 813 Santa Barbara Street, Pasadena, CA 91101

© American Astronomical Society • Provided by the NASA Astrophysics Data System